Electrochemical Heaters Utilizing Aluminum Alloy and Magnesium Anodes

S. Gilman* and P. Bramhall

U.S. Army Electronics Research and Development Command, Electronics Technology and Devices Laboratory, Fort Monmouth, New Jersey 07703

Reprinted from JOURNAL OF THE ELECTROCHEMICAL SOCIETY
Vol. 125, No. 12, December 1978
Printed in U.S.A.

Electrochemical Heaters Utilizing Aluminum Alloy and Magnesium Anodes

S. Gilman* **and P. Bramhall**

U.S. Army Electronics Research and Development Command, Electronics Technology and Devices Laboratory, Fort Monmouth, New Jersey 07703

ABSTRACT

A short-circuited electrochemical cell made with a saline electrolyte, an aluminum alloy or magnesium anode, and a manganese dioxide cathode may be used as a rather efficient short-term portable heater. The use of a magnesium anode provides somewhat higher heat content but results in the production of considerable hydrogen gas. Certain aluminum-zinc alloys are almost as energetic as magnesium and produce little hydrogen.

If an electrochemical cell is short circuited, its chemical energy is almost completely converted into heat via the various ohmic and nonohmic polarizations occurring in the electrolyte at both electrodes. The heat from such an "electrochemical heater" may be largely transferred by thermal conduction to any material with which it is in intimate contact. One advantage of such an electrochemical heat source over a purely chemical (*e.g.*, thermite) one is that the reaction tends to proceed in a more gradual and controlled manner. Compared to the use of an electrochemical cell with a remote resistive heater, the direct electrochemical heater avoids the problem of inefficient transfer of energy from the cell which becomes particularly critical at high rates of cell discharge.

Electrochemical heaters utilizing aluminum and magnesium anodes and various cathodes have been developed for such applications as protective clothing, diving gear, and the heating of field rations (1-4). Magnesium-manganese dioxide cells with saline electrolyte are of particular interest in the last application where it is advisable to avoid toxic materials and where the service life of the heater is of the order of 15 min (4). One disadvantage of the Mg-MnO_2 cell is that a considerable volume of hydrogen is produced during discharge, presenting a potential explosion hazard. Our purpose in this work was to analyze the performance of the short-circuited Mg-MnO_2 cell and determine if similar but hydrogen-free performance could be obtained by substitution of an aluminum alloy for the magnesium.

Experimental

Preparation of electrodes and electrolytes.—Anodes.—The aluminum alloys for these studies were prepared by Reynolds Metals Company using procedures and heat-treatments similar to those previously reported (5). The alloys were prepared with high purity (99.992%) aluminum as a base; the aluminum was induction-melted, in air, in silicon carbide crucibles. All additions of pure metals were made at a temperature over 705°C and stirred to ensure homogeneity. The melts were treated with gaseous chlorine and then semicontinuously cast into ingots using an aluminum direct chill caster. The ingots were cleansed by scalping the surfaces. They were then heat-treated for homogenization and cold-rolled to a thickness of 0.04 cm. Pure aluminum used in half-cell studies was wire of 0.1 cm diam and 99.99+ purity (Alfa Inorganics). Pure magnesium for half-cell studies was 0.3 cm diam rod of "sublime" grade (Dow). The magnesium for whole-cell studies was "primary grade" (Dow) sheet of 0.028 cm thickness. For whole-cell ("electrochemical heater") experiments, 1 × 1 cm anodes were prepared from the appropriate sheet stock by fastening a nickel expanded metal screen (5 Ni 7 — 2/0 from Exmet Corporation) to the back side of the electrode using epoxy cement. The bonding was accomplished in a hydraulic press with heated platens (200 kg/cm² pressure at 135°C). A tab of screen was left on the sample and a heavy gauge tinned copper wire was soldered to it in such a way that no contact was possible between the solder connection and the electrolyte. Samples of flat stock metals used in half-cell experiments were prepared by pressure cementing a nickel foil contact to the top of a 0.5 × 2.2 cm coupon and then masking off the nickel contact with silicone rubber, leaving a 0.5 × 2.0 cm exposed area. Anode surfaces were degreased with trichloroethylene prior to use.

MnO_2 cathodes.—Electrodes were made, or obtained, with various formulations containing MnO_2, graphite, carbon black, graphite fiber, and current-collecting screens. Methods of preparation are reported below for four particular formulations.

(*i*) Electrodes of this formulation were developed (4) and supplied by Power Applications, Incorporated, Valley Stream, Long Island, New York. They were prepared by binding a mixture of MnO_2 (natural ore containing 74% MnO_2), carbon black (Cabot XR-72), and fullers earth (in the weight ratio of 10:2:1), with polytetrafluoroethylene emulsion, to a 20 × 20 mesh steel grid. The completed cathode was of 0.05 cm thickness and contained 0.035g of MnO_2 ore per square centimeter of electrode area.

(*ii*) This formulation was based on formulations reported by Kordesch (6). A mixture of MnO_2 ("chemical MnO_2 ore"), graphite powder, and carbon black (Shawinigan, 50% compressed) in proportions 43:5:1 was ball-milled for 2 hr. The mixture was then blended with fuller's earth and graphite fibers in proportions 100:5:1. The blend was then mixed with a 5% solution of Lucite in trichloroethylene (percentage of Lucite in final dry mixture was 2.5%), applied to an etched 20 × 20 gauge stainless steel screen, and air dried. The completed electrode contained 0.07g of MnO_2 ore per square centimeter of electrode area.

(*iii*) Electrodes of this formulation were developed (6) and supplied by Kordesch (Union Carbide Corporation). They were of similar formulation to the ones described in Ref. (2) above but utilized Tekkosha brand MnO_2, three times the graphite fiber content, and no fuller's earth. The finishing electrodes were 0.1 cm thick and contained 0.17g of MnO_2 per square centimeter of electrode area.

(*iv*) This formulation was prepared using the ball-milled mixture of MnO_2, graphite, and carbon black mentioned in fomulation (*ii*) above. The mixture was dry pressed into a porous nickel matrix (45 pore, 0.41 cm thick "Foametal" from Hogen Industries, Willoughby, Ohio) in a manner similar to that reported

* Electrochemical Society Active Member.
Key words: saline cells, manganese dioxide, corrosion.

previously (7). The final structure was 0.1 cm thick and contained 0.2g of MnO_2 per square centimeter of electrode area.

Electrical contact was made to the cathodes by welding a lead to a tab of exposed screen and insulating in such a way that contact between the lead and the electrolyte was avoided.

Electrolytes.—For experiments with complete flat cells ("electrochemical heater" experiments), the cell was assembled in the dry state, using 0.165 cm thick "Webril R-2801" (Kendall Mills) impregnated with NaCl (0.037 g/cm²) to which water was added just before the experiment. The same electrolyte arrangement was used in the voltage-sweep experiments on cathodes. Experiments on fully immersed anodes and cathodes were performed using a solution of NaCl made by saturating distilled water with reagent grade salt at room temperature.

Procedures for making electrochemical and hydrogen-release measurements.—Electrochemical heater experiments.—Using a 1 × 1 cm anode and cathode, the cells were assembled in a gas-tight Lucite fixture of very small internal volume in which rubber pads maintained pressure on the cell components and acted as a heat sink. The temperature at the anode-rubber interface was monitored with a Chromel-Alumel thermocouple when desired. All the electrodes used in these experiments were fabricated with screens to which heavy current leads were soldered inside the Lucite fixture, and those leads were also useful in supporting and positioning the electrodes in the cell. The cells were fabricated using the salt-filled Webril electrolyte pad described above. The pad was left oversize at one end, and 0.3 cm wide strips of MnO_2 cathode [formulation (i)] were placed in the same planes as the anode and cathode with a 0.1 cm gap between each strip and the adjacent electrode. These served as "dry" reference electrodes for the adjacent anode or cathode. The recorded potentials were then converted to "potentials *vs.* the saturated calomel electrode," by subtracting 0.41V, which takes into account the typical open-circuit voltage of cathode formulation (i). The external connection between the anode and cathode was made by means of a calibrated 0.01Ω shunt through which the "virtual" short circuit current was monitored continuously by means of a strip chart recorder (Hewlett Packard No. 7100B). Simultaneous recordings were made of the anode and cathode potentials relative to their respective reference electrodes. The volume of hydrogen gas evolved from a cell was determined using a gas buret. The dry cell was activated just before use by flooding with water for 15 sec and then draining off the excess.

Measurement of anode polarization and hydrogen gas evolution in half-cells.—Anode polarization was studied using wire or 0.5 × 2 cm foil samples, prepared as specified above. The experiments were performed in a glass-stoppered, thermostated, (25°C) three-compartment cell with a reference saturated calomel electrode (SCE) and a platinized platinum counter-electrode (see Fig. 1). The electrolyte was a saturated solution of sodium chloride; 200 cm³ of the electrolyte were required for the working electrode compartment and that volume was renewed after each determination. The polarization (current-potential) curves were recorded on an X-Y recorder (Hewlett Packard No. 7047A) while applying an anodic potential scan (speed of 0.001 V/sec) using a potentiostat (Tacussel No. P1T20-2A) and signal generator (Tacussel No. GSTP-2). The reverse sweeps were triggered manually after reaching a top current of 200 mA/cm².

Gas evolution was measured for similar anodes under constant-current conditions. The gas evolution measurements were accomplished by means of the glass mantle and bubble flowmeter arrangement shown in Fig. 1. The flowmeter was chosen of either

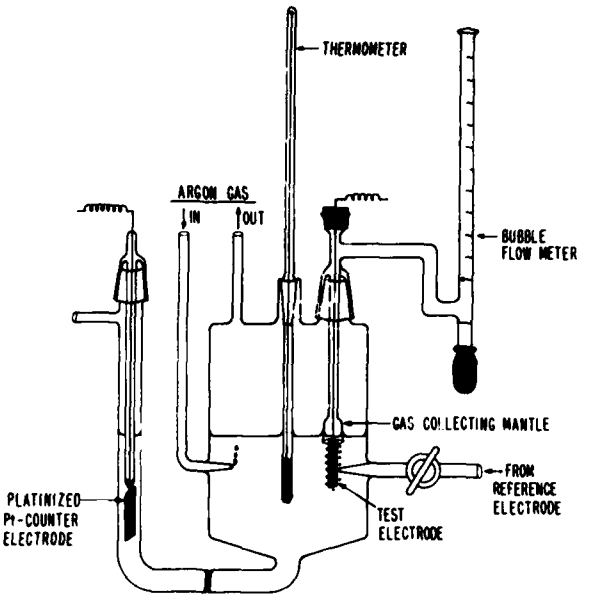

Fig. 1. Glass vessel for polarization and H_2 release measurements

1 or 10 cm³ volume (depending on the anticipated rate of gas evolution) and the position of the bubble recorded at 1 min intervals. With the 1 cm³ flowmeter, flow rates as small as 2.2×10^{-4} cm³/sec (equivalent to an electrochemical H_2 evolution rate of 2 mA) could be read with 90% accuracy within 3 min after initiating the flow, and rates down to 1.1×10^{-4} cm³/sec (1 mA) could be read accurately after 5 min. The accuracy was tested by generating H_2 at a platinum electrode (with 100% efficiency). The 3 and 5 min delay intervals cited above probably correspond to the very slight lowering of the electrode meniscus (the buildup of gas pressure) required to overcome inertia of the soap film in the bubble flowmeter.

Measurement of polarization and hydrogen evolution of fully immersed cathodes in half-cells.—The procedures used for studying MnO_2 cathodes in an excess of saturated NaCl solution were identical to those described directly above for anodes, except for the type of signal impressed on the cathode. In this case, a preselected constant potential was applied to the electrode ("potential-step" method) and the resulting current-time trace was recorded on a strip chart recorder (Hewlett-Packard No. 7100B). A fresh sample of electrode was required for each new potential imposed. Hydrogen gas is evolved at a MnO_2 electrode at sufficiently negative potentials. The rate of gassing was measured under "potential-step" conditions for cathode formulation (1).

Measurement of polarization at cathodes using an electrolyte pad.—For purposes of fast "screening" of new electrolyte formulations, polarization curves were measured using a cathodic potential sweep. Since many of the electrode formulations were found to give better results when mechanically compressed (thus improving contact between the MnO_2 and the current collector), such experiments were performed using the salt-impregnated Webril pad described above, and a Mg "counterelectrode" in an arrangement similar to that described above for "electrochemical heaters."

Results and Discussion

Thermodynamic considerations.—Table I presents the reaction equations and corresponding thermodynamic quantities for the chemical processes antici-

pated in Mg and Al cells utilizing MnO_2 cathodes (8, 9). The standard enthalpy, $\Delta H°$, the standard free energy, $\Delta G°$, those latter quantities divided by the number of equivalents ($\Delta H°/n$ and $\Delta G°/n$), and the standard cell potential $E°$ were calculated using standard enthalpies and free energies of formation (9). Reaction equations for cells 1 and 3 of Table I correspond to coulombically efficient utilization of both plates of each cell. The equations for cells 2 and 4 are for the reactions producing hydrogen. The hydrogen may be produced at either the anode (corrosion) or the cathode (cathode gassing). The most relevant quantities for heat-production purposes are the enthalpies rather than the free energies. Furthermore, reference to the values of $\Delta H°/n$ is useful if we wish to compare the reactions for the same "internal current" of the cell. Since the values of $\Delta G°$ and $\Delta H°$ are almost identical, the values of $E°$ are almost as valid for purposes of comparison as those of $\Delta H°/n$. From the values of $E°$ we may, therefore, conclude that, for identical cell "internal current" and with no hydrogen evolution, the Al/MnO_2 cell is 12% less energetic than the Mg/MnO_2 cell. On the other hand, much of the total "internal current" of the present Mg cell is directed into the far less efficient hydrogen evolution reaction (reaction No. 2, Table I) If this reaction were eliminated, it could more than compensate for the 12% loss.

Thermodynamic reduction potentials for the individual electrode reactions under consideration here are reported in Table II and are discussed later. The standard potentials listed in the table were obtained from Pourbaix's atlas (10).

Polarization and hydrogen gas release at the anode. —In order to best reflect "practical" conditions, anode surfaces were merely degreased and dried before use. Alternative sandpapering of the anode was found to shift polarization curves to more cathodic potentials without changing the relative positions of the various alloys on the potential axis.

For the purpose of screening of a large number of samples, it was convenient to measure anodic polarization using a linear anodic potential sweep. The samples of 2 cm^2 area were fully immersed in a large volume of saturated NaCl solution thermostated at 25°C. The traces of Fig. 2 were obtained by starting at the respective rest potentials and sweeping toward positive potentials at a speed of 0.001 V/sec. Return sweeps

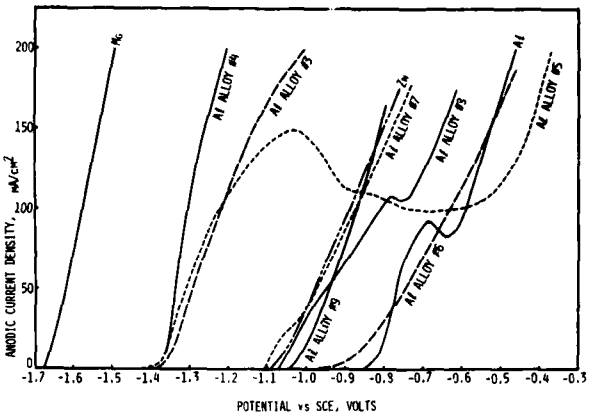

Fig. 2. Anodic polarization curves for several pure metals and aluminum alloys in saturated NaCl solution at 25°C. Alloy compositions are given in Table III.

(in the cathodic direction) were obtained after interrupting the anodic sweep manually at the approximate 200 mA/cm^2 level and then sweeping in the cathodic direction; the resulting traces appear in Fig. 3. A comparison of Fig. 2 and 3 reveals some hysteresis for all of the samples studies. The return sweep for Mg was very similar to the positive-going sweep and is not shown in Fig. 3. The rather pronounced hysteresis for aluminum and its alloys is not surprising considering the fact that aluminum is always covered with a film of γ-Al_2O_3 in near-neutral solutions (5), and that its electrochemical properties depend on the condition of that film, which, in turn, depends on the previous history of the electrode. The behavior of any of the samples, as an electrochemical heater anode, may be expected to fall somewhere between the anodic and cathodic traces, since in such use the current densities are initially high and then undergo gradual decline.

For measurements of hydrogen evolved by the anode samples, it was convenient to impress the various constant current levels listed in Table III. Measurements were made at 1 min intervals for a total of 8 min at each increasing current density. Table III pre-

Table I. Thermodynamic quantities of cell reactions

	Cell	Reaction	$\Delta H°$ (kcal)	$\Delta F°$ (kcal)	$\Delta H°/n$ (kcal/eq.)	$\Delta F°/n$ (kcal/eq)	$E°$ (volts)
1	Mg/MnO_2	$Mg + 2MnO_2 + H_2O \rightarrow Mg(OH)_2 + Mn_2O_3$ (β-form) (α-form) (α-form)	−135.8	−133.5	−67.9	−66.8	2.88
2	Mg/H_2	$Mg + 2H_2O \rightarrow Mg(OH)_2 + H_2$	−84.4	−85.9	−42.2	−43.0	1.86
3	Al/MnO_2	$2Al + 6MnO_2 + H_2O \rightarrow Al_2O_3 \cdot H_2O + 3Mn_2O_3$ (β-form) (Hydrated γ-form) (α-form)	−351.9	−351.0	−58.7	−58.5	2.54
4	Al/H_2	$2Al + 4H_2O \rightarrow Al_2O_3 \cdot H_2O + 3H_2$ (Hydrated γ-form)	−197.7	−208.2	−33.0	−34.7	1.50

Table II. Thermodynamic reduction potentials at 25°C

	Electrode reaction	Standard potential† (volts)	Reversible potential vs. SCE (volts)		
			pH 6.1*	pH 7.0	pH 10.45**
a	$2MnO_2 + 2e^- + H_2O \rightleftharpoons Mn_2O_3 + 2(OH^-)$ (β-form) (α-form)	1.014-0.0591 pH	0.417	0.364	0.160
b	$2H_2O + 2e^- \rightleftharpoons H_2 + 2(OH)^-$	−0.0591 pH	−0.591	−0.650	−0.853
c	$Mg(OH)_2 + 2e^- \rightleftharpoons Mg + 2(OH^-)$	−1.862-0.0591 pH		−2.512	−2.715
d	$Al_2O_3 \cdot H_2O + 3H_2O + 6e^- \rightleftharpoons 2Al + 6(OH^-)$ (Hydrated γ-form)	−1.506-0.0591 pH	−2.102	−2.156	

† Standard potentials are referenced to the normal hydrogen electrode.
* The pH of a saturated solution of γ-aluminum oxide is 6.1.
** The pH of a saturated solution of $Mg(OH)_2$ is 10.45.

Table III. Hydrogen evolution at magnesium, aluminum, and aluminum alloy anodes (25°C)

Composition No.	Anode composition (w/o)							Percentage H_2 evolution* (I, mA/cm²)					
	Mg	Al	Zn	Hg	Sn	Ga	In	5	10	20	50	100	200
1	100							43.6		45.3		38.7	36.9
2		100								13.4	16.9	19.8	15.9
3	0.57	99.25			0.13	0.05			8.6		16.8	16.3	6.9
4	0.82	99.98			0.15	0.05			17.7	14.1	14.5	13.8	
5	0.36	99.44			0.14	0.06			20.4	15.6	13.2	11.4	10.6
6		98.52	1.47	0.01						12.5	11.3		13.2
7	0.46	95.31	4.19				0.04				0.6	1.4	1.5
8		96.45	3.52				0.03				5.5	2.6	2.0
9		95.81	4.19						4.0	16.7	20.1	16.3	

* Percentage H_2 evolution = $100\ I_{H_2}/(I + I_{H_2})$.

sents the hydrogen evolution rate as a percentage of the total current at the anode after converting the gassing rate to an equivalent current density, I_{H_2}, by using the formula

$$I_{H_2} = 2 \cdot \frac{\Delta V}{\Delta t} \cdot \frac{F}{22.4} \qquad [1]$$

Where F is the Faraday constant and I_{H_2} is obtained in amperes/cm² if the gas flow, $\Delta V/\Delta t$, is expressed in liters per second per square centimeter of electrode area.

For current densities of 20 mA/cm² or higher, the gassing rates were found to stabilize after 2-3 min and the values given are average values for the last 4-8 min of observation. Since direct calibration revealed that a 2-3 min lag is inherent in the flowmeter used for the measurements, no conclusions may be drawn about intrinsic transient behavior of the system in that early period. For the alloys possessing low rates of gassing, the method was not sufficiently sensitive for observations to be made in the allotted time at the lowest current densities.

Referring to Fig. 2 as a guide to the relative anodic behavior of the various anode materials, we see that the polarization of the alloys falls into the approximate 1V span between Mg and pure Al, with the latter the more inactive material and with both operating much below their respective thermodynamic potentials, as listed in Table II. A trace for a Zn electrode is incuded for comparison, although the energy content of Zn is too low for practical consideration. A general pattern of behavior emerges for the alloys if the high current performance of alloy No. 5 is ignored. Those alloys (No. 3, 4, and 5) containing Sn produce the most negative (active) closed-circuit voltages. This is in agreement with observations (5, 11) made during long-term corrosion studies on aluminum alloy/steel couples. It is believed (11) that Sn fosters the high anodic activity by producing cation vacancies which reduce the ionic resistivity of the γ-alumina film. This film normally covers the electrode during use. Additions of Mg and Ga enhance this effect by stabilizing the solid solubility of the Sn in the alloy (12). The H_2-evolution characteristics of alloys No. 3-5 tend to be somewhat better than that of pure Al, particularly at the high current densities, and like Al, are a 2-3 fold improvement over Mg in that regard. A second grouping of Al alloy polarization traces fall between the trace for pure Al and pure Zn (Fig. 2). Alloys 6-9 contain increasing amounts of Zn, and their closed circuit voltages, in line with previous experience with Al-Zn alloys (11), tend to become increasingly more negative and approach the performance of a pure Zn anode. There is, however, no simple correlation between electrode polarization and hydrogen evolution for this series of alloys, if the results of Fig. 2 and Table III are compared. Specifically, alloys No. 7 and 9 have the same Zn content and show very similar polarization behavior, but in spite of these facts alloy No. 7 produces the lowest amount of hydrogen while hydrogen production for alloy No. 9 falls in the same range as for pure aluminum. The fact that alloy No. 8, like alloy No. 7, is also a low gas producer, suggests that indium is more significant than Mg in imparting the nongassing properties to those alloys. Before considering how alloying affects hydrogen evolution, let us consider the thermodynamics of the process. For gassing to occur at all, the electrode potential must be more negative than the thermodynamic value for a reversible H_2 electrode in the same medium. According to Table II, that potential

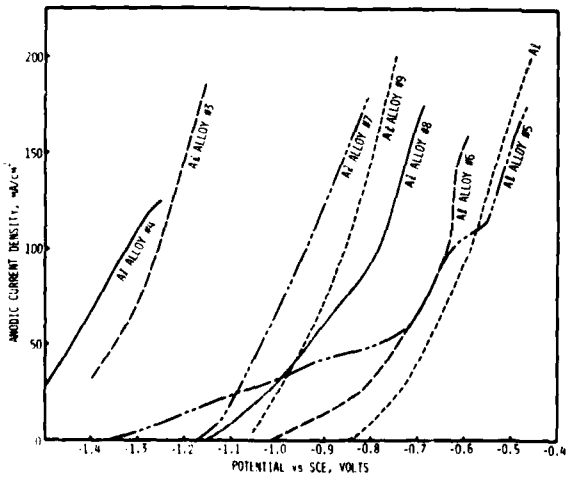

Fig. 3. Anodic polarization curves for several pure metals and aluminum alloys in saturated NaCl solution at 25°C. The curves were obtained after reversing the linear potential sweeps of Fig. 1.

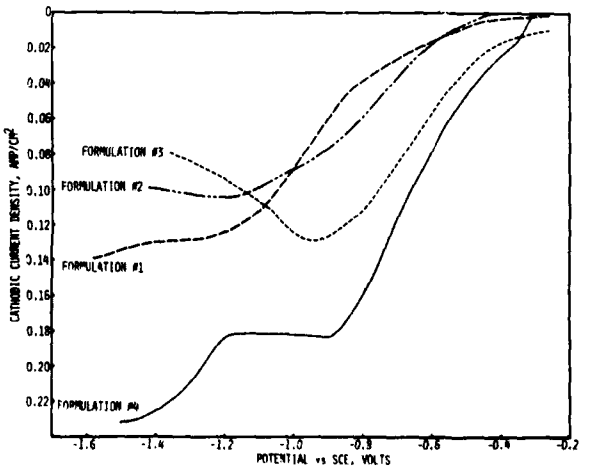

Fig. 4. Cathodic voltage scans of various MnO_2 cathodes. The electrolyte was NaCl solution in a Webril Pad.

could be −0.650V in the original neutral solution and −0.591V at steady state, with the solution completely equilibrated and saturated with hydrated γ-aluminum oxide. Based on those numbers, gassing would not be expected on pure Al or on alloy No. 6 at the higher current densities. However, localized, very low *p*H values may be expected near the anode surface, particularly at high current densities, corresponding to the production and hydrolysis of $AlCl_3$. For example, based on the reported value of $pKh = 4.9$, the *p*H of a 1M solution of $AlCl_3$ would be 2.45 and the corresponding reversible H_2 potential would be −0.38, sufficiently positive to account for H_2 evolution on Al and all of its alloys in a sodium chloride electrolyte solution. As for Mg, Table III reveals that the percentage of hydrogen evolved does not generally or systematically drop as the current is raised and the potential approaches that of the reversible H_2 electrode ("negative difference effect") (13). As for Mg, therefore, it may be hypothesized that H_2 release occurs on a very limited, momentarily film-free fraction of the surface. In line with that concept, the role of indium in a Zn-Al alloy could be to modify the physical structure of the film (*e.g.*, adherency, coherency, porosity) so as to minimize exposure of bare surface to the electrolyte.

We shall now turn to the problem of choosing the "best" anode material for an electrochemical heater. From the point of view of lowest H_2 production, Table III reveals that alloy No. 7 appears to be the best choice, with No. 8 a close second choice. Assuming that the solid product of reaction is γ-alumina for both Al and all of the Al-rich alloys, the total heat produced per equivalent of Al consumed in short-circuited cells utilizing any of those anodes and a MnO_2 cathode should be greater for the alloys producing the least H_2 (since reaction 3 of Table I is more energetic than reaction 4). So far, the analysis has been based on thermodynamic and corrosion data only. The role played by anode polarization is discussed later.

MnO_2 cathode polarization and gas evolution at the cathode.—The polarization of a manganese dioxide cathode at high rates of discharge is much more time dependent than that of the Mg and Al anodes with which it might be used. Because of the strong time-dependence, measurements of polarization performed at fixed potential provide the most quantitative guide to performance of the electrode in an electrochemical heater. For this purpose, electrodes of formulation No. (*i*) measuring 1 × 1 cm were individually immersed in a saturated solution of NaCl. The area of each sample is taken as 1 cm^2 despite the fact that both sides are exposed, since the bulk of the porous cathode is utilized rather than its surface (the reverse is true for anodes). For each sample, a different fixed potential was applied and the current-time trace recorded. Points taken from the traces are plotted on Fig. 5. From the figure it can be seen that, for time durations at constant potential of less than 1 min, the current tends to increase with decreasing potential. For longer time durations, a plateau value occurs in the lower potential range. A second rise in current follows the plateau at decreasing potentials. The results can be interpreted as follows, based on the observation (14) that the cathodic reduction of MnO_2 tends to be diffusion-controlled soon after the beginning of the process:

(i) At short elapsed time, including up to 12 sec, the reduction is only partially diffusion limited and hence shows considerable potential dependence over the whole potential range.

(ii) After sufficient charge has passed, the reduction process becomes solid state diffusion controlled and, therefore, exhibits a current plateau. Referring to the 1 min points, a plateau is evident from −1.0 to −1.5V. At less cathodic potentials than −1.0V, the previous activation-controlled current was not sufficiently high to result in diffusional control after 1 min. At more cathodic potentials than −1.5V, the current rise is due to electrolytic evolution of H_2.

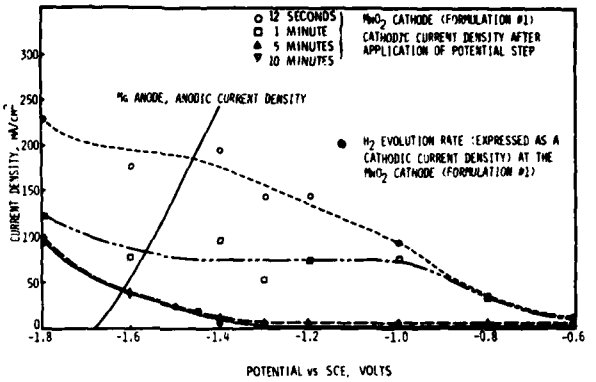

Fig. 5. Polarization behavior of fully immersed Mg anodes and MnO_2 cathodes [formulation *(i)*] in saturated NaCl solution.

(iii) As the reduction time increases, diffusional control extends to less cathodic potentials, and the onset of H_2 evolution is more easily distinguished (potentials as positive as −1.3V).

To confirm that hydrogen is evolved at the more cathodic potentials, a sample of electrode was first prepolarized at −1.4V for 10 min. The potential was then adjusted to any desired value and gas evolution was measured. The gas evolution rates (measured at 100 sec intervals) were found essentially time independent, as might be expected for an electrocatalytic process. Average rates, converted to currents by means of Eq. [1], are plotted on Fig. 5. The results reveal that H_2 evolution is measurable at −1.3V and it accounts for virtually all of the cathodic current at more cathodic potentials after a few minutes of polarization. The reversible potentials (*vs.* a saturated calomel electrode) of the two processes, which may occur at the MnO_2 cathode, appear in Table II (*i.e.*, a and b). The expressions for the standard potentials were taken from Ref. (10). The *p*H of the NaCl electrolyte should be 7.0 initially, and should eventually reach 10.45 when thoroughly mixed and saturated with $Mg(OH)_2$ (10). In addition, transient high and low values of *p*H at the cathode and anode, respectively, are likely during high current surges. Since the reversible potentials from Table II for reaction a at *p*H's 7 and 10.45 are quite positive, it is apparent that MnO_2 (Fig. 5) is being reduced irreversibly and that improved reduction kinetics would shift the curve to the right on the potential axis. For the H_2-evolution process (reaction b, Table II), it can be seen that gas evolution could begin at potentials as positive as −0.65V. The observation that no appreciable gassing occurs until −1.3V largely reflects the fact that carbon (which is present for its electronic conduction properties) is a poor electrocatalyst for the hydrogen evolution reaction.

From Table II it can be seen that the reversible potential of the MnO_2 electrode is +0.364V in the originally neutral solution used here as the electrolyte. Variations in *p*H during cell discharge can be expected to affect the reversible potential by only a few tenths of a volt. In spite of this, "formulation No (*i*)" begins to deliver appreciable cathodic currents at potentials over a volt more cathodic than the reversible potential. Such irreversible performance is subject to improvement through structural modifications which decrease internal impedances and improve mass transport in the electrode. Toward that end, a number of different electrode formulations were made for evaluation. These formulations included variation in: (i) the amount of carbon and graphite added for contact between MnO_2

particles; (ii) nature of the organic binder (*e.g.*, PTFE, Lucite, polysulfone); (iii) addition of agents to increase wetting and porosity (*e.g.*, fuller's earth) nature of the current collector (*e.g.*, screens and expanded metal made of steel and nickel), and (iv) the addition of graphite fibers to improve current collection.

For evaluation of samples, the potential-step method, as used to obtain the data of Fig. 5, provides the most in-depth information, but requires multiple samples and is tedious. Therefore, for the present purpose of fast screening, the linear potential sweep method requiring only one sample for a determination was used instead (sweep speed of 0.001 V/sec). Samples of 1 × 1 cm dimensions were discharged against a Mg counter electrode using a NaCl-impregnated Webril separator pad as the electrolyte. Some of the more promising results appear in Fig. 4. Formulation No. (ii)-(iv) all offer the promise of improved performance at more positive potentials as compared with formulation No. (i). All three improvements utilize graphite fiber additions. Formulation No. (ii) and (iii) were made with a steel screen current collector, while No. (iv) was made with a "foametal" current collector. While cathode performance increases on progressing from formulation No. (i)-(iv) so does the MnO_2 loading (0.035, 0.07, 0.17, and 0.2 g/cm² for electrodes 1, 2, 3, and 4, respectively). Hence, the improvement represents successful utilization of more MnO_2, rather than a fundamental improvement in the kinetics of MnO_2 reduction. From Fig. 4, formulation No. (iv) would appear to be the obvious choice for further development. Its vulnerability, however, lies in the fact that Ni is a rather good catalyst in the H_2 evolution reaction. The descending portion of the scan from −1.2V to more cathodic potentials corresponds largely to extensive gas production, which is significant even at more positive potentials. An electrochemical heater using that formulation was nevertheless evaluated and the results are reported in the section below. Formulation No. (iii) appears clearly superior to formulation No. (i) without an aggravated gas evolution problem, and its further evaluation is also reported in the section below.

Electrochemical performance and hydrogen release at a short-circuited Mg-MnO_2 cell.—The behavior of a "heater" utilizing a Mg anode will serve as an example of the more general case. The results appearing in Fig. 6 were obtained for a cell containing a 1 × 1 cm anode and cathode and a salt-impregnated Webril separator. The "virtual" short-circuit current (across a 0.01 Ω load) density and the individual electrode potentials (referred to a saturated calomel electrode) were recorded after activating the cell by flooding with water for 15 sec and then draining off the excess water. The volume of hydrogen released was measured periodically and converted to an equivalent current density, I_{H_2}, using Eq. [1]. I_{H_2} includes a contribution from both the anode and cathode. The initial large values of I_{H_2}, paralleling the large values of I_{sc}, correspond mainly to hydrogen release at the anode, whereas the longer-term smaller values of I_{H_2} correspond to cathodic release of hydrogen as is discussed below. For the early large currents, the areas under the two curves are approximately measures of the number of equivalents of Mg reacting according to the equations in cells 1 and 2, respectively, of Table I. The initial high surge of current is useful for providing rapid heat transfer. By minimizing the masses of the ingredients, practical cells (4) transfer most of the available enthalpic heat to the object being heated.

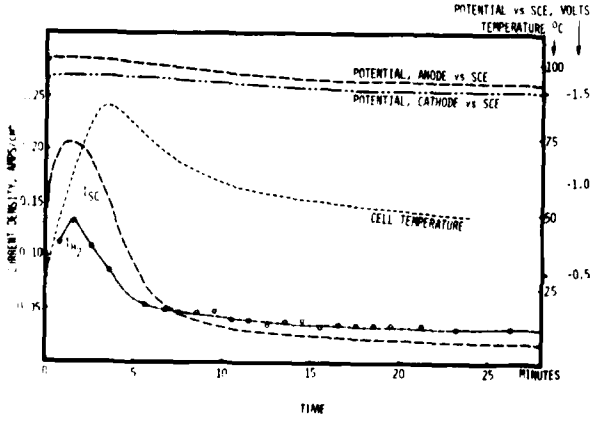

Fig. 6. Operating characteristics of an instrumented Mg/MnO_2 electrochemical heater [cathode formulation No. (i)].

Although the respective experimental conditions are somewhat different, the electrode polarization results of Fig. 5 are useful in qualitative interpretation of the results recorded in Fig. 6. For a short-circuited cell consisting of the anode and cathode of Fig. 5 and with negligible electrolyte resistance, the short-circuit current and electrode potential at any instant are determined by the point of intersection of the Mg anodic polarization curve with the appropriate MnO_2 cathodic polarization curve. The intersections of Fig. 5 predict a drop in current from the 200 mA/cm² level in the first 12 sec, to below the 50 mA/cm² level in 10 min, with that sharply declining current attributable entirely to cathode polarization. The long-term currents (according to Fig. 5) are supported almost entirely by hydrogen evolution. Finally, Fig. 5 predicts a moderate shift in the electrode potentials to more cathodic potentials, conforming to the shape of the anodic polarization curve. This predicted shift occurs during the first few minutes for the more complicated conditions of Fig. 6. The unanticipated long-term positive drift of potentials probably corresponds to electrode polarizations due to the limited volume and shifting pH of the electrolyte in the Webril pad in use here. The short-circuit current (I_{sc}) *vs.* time trace of Fig. 6 exhibits approximately the expected type of current decay after the current peak is passed. The initial rise in current probably corresponds mainly to the "voltage delay" phenomenon normally encountered (15) when a heavy load is first applied to the normally passive Mg anode.

A very significant conclusion based on Fig. 5 is that shifting of the anodic curve to the right would tend to eliminate H_2 evolution at the cathode, the latter being the major source of H_2 evolution after the first 10 min of cell operation.

With the help of Fig. 5, we can return to the problem of choosing the "best" Al alloy to substitute for Mg. In addition to the preference for the lowest corrosion rate, the polarization of the anode plays an important role in three important ways:

(i) The distribution of heat through the cell depends on the relative extents of anode and cathode polarization and of electrolyte resistance. For reasons of heat conduction it is best to place the work against the metallic anode and it is therefore beneficial to have the highest polarization (and temperature) at that electrode.

(ii) The rate of heat release is proportional to the current density. That rate (or current) depends on the points of intersection of the anode and cathode polarization curves, and will be highest for those anode polarization curves falling closest to that of Mg.

(iii) The anode polarization curve helps establish the working potential of the cathode at short circuit. The more positive the anode potentials (and the cathode working potential), the more likely will be the avoidance of H_2 evolution at the cathode. The latter has already been shown to be largely responsible for

longer-term gas evolution. Considerations (*i*) and (*iii*) suggest that the polarization curve of the anode should be as far as possible to the right of that of Mg (*e.g.*, the low-gassing alloy No. 7 of Fig. 2). The problem of lower current densities than for Mg [consideration No. (*ii*)] can be overcome by improvement of the cathode. Figure 5 suggests that other cathode formulations [No. (*iii*) and (*iv*)] might provide superior performance in an electrochemical heater utilizing aluminum alloys because of the significant shift of the polarization curve to the right on the potential axis.

Electrochemical performance and hydrogen release at short-circuited aluminum.—Alloy-MnO_2 Cells.—Figures 7-9 present results for short-circuited cells utilizing an aluminum alloy and three differently formulated MnO_2 cathodes. The plot of I_{sc} *vs.* time for the Mg-MnO_2 cell of Fig. 6 is included for comparison. Figure 7 confirms the expectation that relatively poor results can be obtained with an aluminum alloy anode if the cathode will not support high currents at the more positive potentials. Figure 8 reveals that an improvement in current densities over the Mg-MnO_2 cell can be achieved with an aluminum alloy if the MnO_2 cathode has improved performance at low overvoltages. As anticipated, I_{H_2} is much lower initially than for the Mg cell, corresponding to low corrosion of the alloy. Since the cathode now operates at relatively positive potentials, there is no significant evolution of

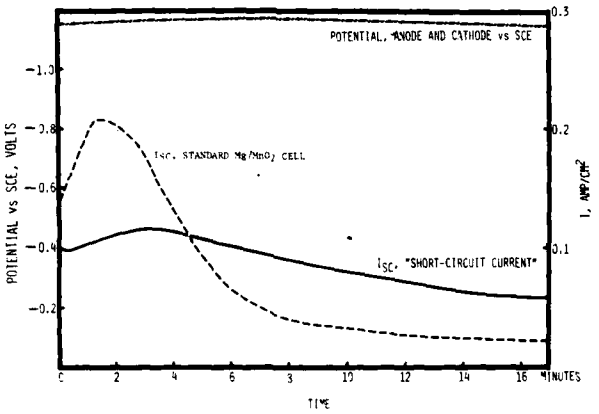

Fig. 7. Operating characteristics of an electrochemical heater made with an Al alloy No. 7 (4.19% Zn, 0.04% In, 0.46% Mg) anode and a MnO_2 formulation No. (*i*) cathode.

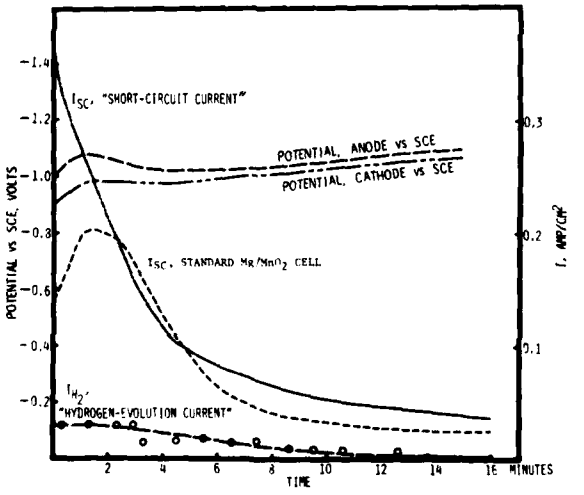

Fig. 8. Operating characteristics of an electrochemical heater made with an alloy No. 7 (4.19% Zn, 0.04% In, 0.46% Mg) anode and a MnO_2 formulation No. (*iii*) cathode.

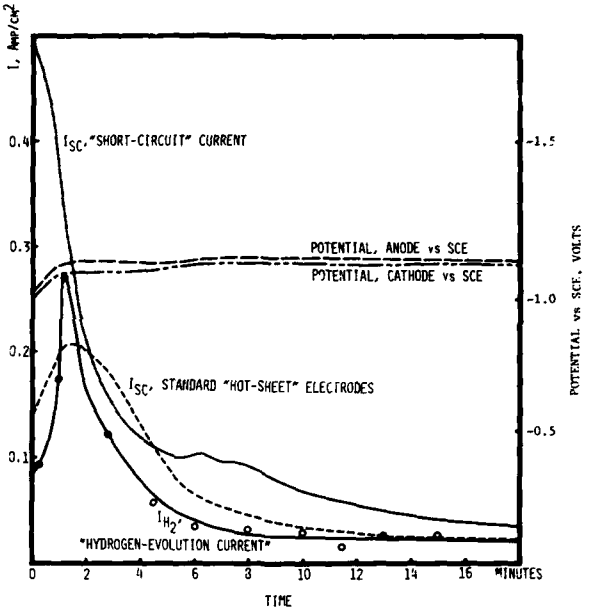

Fig. 9. Operating characteristics of an electrochemical heater made with an Al alloy No. 7 (4.19% Zn, 0.04% In, 0.46% Mg) anode and a MnO_2 formulation No. (*iv*) cathode.

hydrogen gas there. Hence, production of H_2 eventually drops to very low values parallelling the drop of cell current and rate of corrosion of the aluminum at the anode.

From Fig. 9, even more impressive short-circuit currents are obtainable using cathode formulation No. (*iv*), but I_{H_2} is unexpectedly high. It appears that this results from the use of nickel in the cathode formulation, resulting in catalysis of the hydrogen evolution reaction at both anode and cathode.

Conclusions

The nontoxicity and high enthalpic content of saline Mg-MnO_2 and Al-MnO_2 cells makes them useful as electrochemical heaters (short-circuited cells). The Mg cell provides high short-circuit currents (and rates of heat evolution) but produces H_2 at the anode (corrosion) and at the cathode (due to highly negative operating potential). Cells made with certain Al-Zn alloys also provide high short-circuit currents while producing little H_2 at the anode and virtually no H_2 at the cathode (latter due to relatively positive operating potential).

Acknowledgments

The authors wish to thank Dr. Kwoh H. Hu, of the U.S. Army Natick Laboratories, for inspiring this work and for helpful discussions. Support of this work by the Natick Laboratories is gratefully acknowledged.

The authors wish also to thank Drs. D. Thompson of the Reynolds Metals Company and K. V. Kordesch of the Union Carbide Corporation for helpful discussions and samples of the anode and cathode materials discussed herein.

Manuscript submitted Jan. 10, 1978; revised manuscript received June 31, 1978.

Any discussion of this paper will appear in a Discussion Section to be published in the June 1979 JOURNAL. All discussions for the June 1979 Discussion Section should be submitted by Feb. 1, 1979.

Publication costs of this article were assisted by the U.S. Army Electronics Command.

REFERENCES

1. W. C. Spindler, U.S. Pat. 3,207,149 (1965).
2. F. P. Kober, U.S. Pat. 3,774,589 (1973).

3. J. F. McCartney, U.S. Pat 3,884,216 (1975).
4. Final Tech. Rep. No. 74-44-GP by Power Applications Inc. on Contract No. DAAG-17-73-C-0250 with The General Equipment and Packaging Laboratory, U.S. Army Natick Laboratories (1973).
5. D. S. Keir, M. J. Pryor, and P. R. Sperry, *This Journal*, **114**, 777 (1967).
6. K. Kordesch, U.S. Pat 3,945,847 (1976).
7. H. F. Hunger and J. E. Ellison, *This Journal*, **122**, 1288 (1975).
8. "The Primary Battery," Vol. 1, G. W. Heise and N. C. Cahoon, Editors, John Wiley & Sons, Inc., New York (1971).
9. "Handbook of Chemistry and Physics," 53rd ed., Chemical Rubber Co., Ohio (1972).
10. M. Pourbaix, "Atlas of Electrochemical Equilibria in Aqueous Solutions," Pergamon Press, New York (1966).
11. J. T. Reding and J. J. Newport, *Mater. Prot.*, Dec., p. 15 (1966).
12. D. S. Keir, M. J. Pryor, and P. R. Sperry, *This Journal*, **116**, 319 (1969).
13. J. L. Robinson and P. F. King, *ibid.*, **108**, 36 (1961).
14. F. Kornfeil, *ibid.*, **109**, 349 (1962).
15. J. L. Robinson, in "Proceedings of the 17th Annual Power Sources Conference," p. 142, May 1963.